Optical properties of DNA-hosted silver clusters

Markesevic, N.

CHAPTER 2

Spectral Properties of Individual DNA-Hosted Silver Nanoclusters at Low Temperatures

In this Chapter the first single emitter fluorescence spectra of DNA-stabilized silver clusters (Ag:DNAs) at ambient and cryogenic temperatures are presented. While Ag:DNAs have received much attention recently due to their sequence-tunable emission wavelengths, the nature of the optical transitions (molecule-like or collective, cluster-like) is an open question. By removing the ensemble broadening present in previous spectroscopic studies, we probe the line widths Γ and brightness of individual Ag:DNA emitters. A roughly 5-fold increase in brightness from 295 to 1.7 K is accompanied by a factor of 2 decrease in Γ. The symmetric emission line shape, its sensitivity to embedding medium, and the independence of emission wavelength on excitation energy together indicate that the measured Γ represents the homogeneous line width, while the large, $\sim$ 100 meV values of Γ suggest rapid dephasing of a collective excited state of the silver cluster.

This Chapter is based on: S. S. R. Oemrawsingh, N. Markešević, E. G. Gwinn, E. R. Eliel, D. Bouwmeester, *Spectral properties of individual DNA-hosted silver nanoclusters at low temperatures*, J. Phys. Chem. C **116**, 25568 (2012).

2.1 Introduction

Nanoclusters of noble metals bridge the gap between the atomic and nanoparticle (plasmonic) regimes. They typically consist of a few to tens of atoms, corresponding sub-nanometer sizes comparable to the Fermi wavelength ($\sim$ 0.5 nm in Ag and Au). In this quantum size regime, nanoclusters possess interesting chemical and physical properties [37]. The strong fluorescence exhibited by silver nanoclusters [38, 39], and the fact that their absorbance and fluorescence spectra depend strongly on cluster size and shape [40, 41], is a striking example. The potential to size-tailor these properties for use in solution or solid state has motivated extensive efforts to develop strategies for chemical stabilization of quantum-sized noble metal clusters. In recent years, a wide range of ligands has been employed to stabilize clusters of both gold and silver, including dendrimers, various functionalized amino acids and thiols, and biological matrices [6, 10, 42–46]. Because most of the atoms in nanoclusters are at its surface, the ligands controlling the cluster size can potentially alter the electronic states that dominate optical transitions to involve both ligand and cluster orbitals, thereby changing the optical properties of the ligated cluster. Understanding and exploiting the effects of the ligand environment on the optical properties of metal nanoclusters, particularly the poorly understood but empirically important effects of ligand choice on fluorescence, is the focus of current research [47, 48].

DNA-stabilized silver nanoclusters (Ag:DNAs), the subject of this Chapter, are drawing increasing interest due to their sequence tunable fluorescence wavelengths, as well as the high quantum yields and good photostability shown by some specific Ag:DNAs [10, 13, 49–54]. Recently demonstrated applications include advanced biological imaging [17], molecular logical schemes [55], and sensors for single base mutations [14], miRNAs [56], and metal ions [16]. Of particular interest is the wide spectral range spanned by fluorescent Ag:DNAs that form on various host strands [10, 51, 52, 57], covering the visible through the infrared. This large color space offers the potential to encode positional information as wavelength, by anchoring Ag:DNAs to DNA scaffolds [33] or incorporating them into living cells [17], In such applications, the line width of individual Ag:DNAs will limit the number of spectrally distinct color channels.

Advances in techniques for isolating specific Ag:DNA comlexes have

recently enabled identification of the numbers of silver atoms in several Ag_n:DNAs, with n from 10 to 24 and emission wavelengths from 500 to 800 nm [53]. For the same 10-24 atom size, the dominant optical transitions of ligand-free clusters are collective in nature (plasmon-like) [58]. However, previous reports on Ag:DNA have considered them to be molecular in character. The distinction becomes important when considering line widths. The single-electron excitations of isolated molecules are usually spectrally narrow, but the collective excitations of multiple, delocalized electrons are subject to broadening by intrinsic dephasing processes [59–62]. These are well-understood for larger metal clusters but have been little explored in the quantum size regime [59, 61].

In this work, we report on the first spectroscopic measurements of Ag:DNA on the single-emitter level at ambient and low temperatures, and determine their fluorescent line width. To our knowledge, this has not previously been determined for ligand-stabilized noble metal clusters in the quantum size regime. In the limit of low temperatures, where vibronic degrees of freedom are mostly frozen out, the remaining spectral line shape and width of a single Ag:DNA will provide important information on whether the optical transitions have a cluster-like, collective, or molecule-like character.

To develop Ag:DNAs that are excitable within the 575-595 nm spectral range of the dye laser used for these studies, we carried out preliminary solution fluorescence studies of Ag:DNAs synthesized on some dozens of different DNA strands. We selected the strands used in this study, 5′-CCG-CCA-CCC-CGC-GGT-3′ (DNA1) and 5′-CCG-CCC-CCC-TGC-GGT-3′ (DNA2), on the basis of their relatively bright emission from bulk solution under excitation within that wavelength range. DNA1 differs from DNA2 by a two-base mutation that produces distinct spectral properties.

2.2 Experimental methods

Synthesis of the fluorescent Ag:DNAs is identical for both oligomers. The DNA strands (Integrated DNA Technologies) are hydrated in ammonium acetate buffer (99.999%, Sigma Aldrich), and subsequently, $AgNO_3$ (99.9999%, Sigma Aldrich) is added to the solution. After $\sim$ 15 min, a freshly prepared solution of the reducing agent $NaBH_4$ (99%, Sigma Aldrich) is added. Final concentrations were 50 μM DNA, 350μM AgNO3, 100 μM NaBH4, and 20

mM ammonium acetate. All solutions were prepared with nuclease-free water (Integrated DNA Technologies). The Ag:DNA samples are used without further purification.

The sample solutions are spectrally characterized in the visible regime (400-800 nm) with a Cary Eclipse fluorimeter (Varian), at a DNA concentration of 25μM. This is achieved by diluting either with nuclease-free water or with the medium, poly(vinyl alcohol) or glycerol, in which we suspend the Ag:DNAs for low-temperature studies.

To achieve the high photon fluxes needed for single emitter studies of Ag:DNAs, we used a sub-GHz-line width ring dye laser (Coherent 899) with Rhodamine 590 Tetrafluoroborate dye (Exciton). The excitation light is filtered with a short-pass filter (edge at 600 nm), to remove weak emission from the laser that is redder than the main excitation peak, which would otherwise generate a large spectral background. The excitation and emission paths are separated by a dichroic mirror (edge at 600 nm). The emission path contains an additional long-pass filter (edge at 600 nm), to exclude residual excitation light. This setup provides a usable excitation range of 575-595 nm. Fluorescence spectra were recorded with a thermoelectrically cooled fiber-coupled spectrometer (Ocean Optics QE65000) that has a spectral resolution of ~ 1.5 nm. The integration time was set at 60 s. Use of a cooled CCD camera (Ikon-M 934-BRDD, Andor Technology) enabled us to take images of single emitters, using a custom cryogenic objective assembly in the helium sample space of our cryostat, with a total magnification of 120X. Finally, we measured intensity fluctuations from single Ag:DNA emitters by using a fiber-coupled single-photon counting module (SPCM-AQR-14-FC, Perkin-Elmer).

For low-temperature ensemble measurements, the sample is diluted to a 25 μM DNA concentration, by adding a 50% (by volume) solution of glycerol. The glycerol ensures that a high quality optical glass forms at low temperatures, by preventing the formation of small, light-scattering ice crystals. We found that the glycerol reduced the emission brightness by a factor of 3 or more and thus significantly reduced the signal-to-noise ratio, making it a poor host medium for single-emitter measurements. Therefore, most single-emitter measurements were made on Ag:DNAs that were spin-cast onto a fused silica substrate from a dilute solution of poly(vinyl alcohol) (PVA). The PVA forms a robust film for cryogenic measurements. To prepare samples for single-emitter studies, the Ag:DNA solution is diluted to a concentration

of 20 nM in a 5 mg/ mL solution of PVA (98%, 16 kD, Acros Organics). The Ag:DNA and PVA solution is then spin-coated for 90 s at 4000 rpm onto a fused silica substrate. Ensemble measurements on Ag:DNA in PVA showed no decrease in fluorescence brightness, consistent with previous measurements [51]. The single-emitter line shapes, widths, and wavelengths did not change significantly when embedded in either PVA or glycerol.

For the low-temperature measurements, the sample is placed in a custom-built helium-bath cryostat. The temperature of the liquid helium is then lowered below the helium lambda point to 1.7 K, by pumping on the bath. This is crucial for the measurements, as it suppresses the formation of bubbles associated with the boiling of the liquid helium, which would otherwise scatter the light. Due to changes in alignment that result from thermal contraction during cooling, it was not possible to reliably track a particular emitter during cool-down. The result is that spectra at room temperature and at low temperature are taken for different individual emitters.

2.3 Results

After synthesis of the Ag:DNAs, we first characterize the fluorescence by recording the excitation and emission spectra in solution, at room temperature. In Figure 2.1, the fluorimetry results are shown, where the horizontal and vertical axes indicate the excitation and emission wavelengths, respectively, and the coloring represents the intensity detected in the emission path. The figure shows that the Ag:DNA2 sample has two fluorescent peaks, while the Ag:DNA1 sample has three, all at different spectral locations. As such, Figure 2.1 visualizes that the nucleotide sequence indeed influences the spectral distribution of the Ag:DNA emitters that form on different strands, as has been reported previously [13]. Each peak represents a different fluorescent species, which is typically defined by the size of the silver cluster and the folding of the Ag:DNA molecule as a whole [50, 51].

In our study, we concentrated on the Ag:DNA1 emitters that excite near 565 nm and fluoresce near 620 nm, and the Ag:DNA2 emitters that excite near 605 nm and fluoresce near 685 nm, because these emitters lie close enough to the 575-595 nm laser range to be excited. Prior studies of Ag:DNAs with known composition identified a trend to longer emission wavelengths for larger numbers of silver atoms [53]. Based on this trend, we infer that the

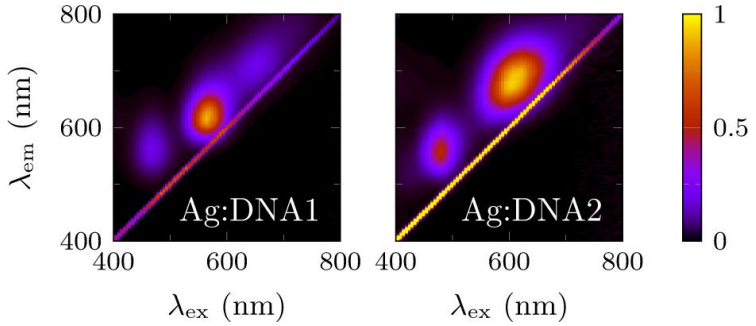

Figure 2.1: Fluorimetry results of Ag:DNA1 and Ag:DNA2 ensembles in solution at room temperature. Excitation and emission wavelengths are plotted along the horizontal and vertical axes, while the color indicates the detected intensity. The diagonal is caused by scattered excitation light.

Ag:DNA1 and Ag:DNA2 emitters contain 14-16 silver atoms. The prior finding that there is a systematic relation between color and silver atom number suggests that the actual cluster size scales with the total Ag content; however, the specific arrangement (geometry and degree of coordination) are not known.

At room temperature in solution, the emission lines are typically broadened by effects such as collision of the emitters with solvent molecules, fluctuating polar interactions with the solvent, and thermal excitation of vibronic states. It has been suggested that isomer interconversions of ~ 10 atom silver clusters may also be a source of line broadening at room temperature [63].

In solution, an ensemble of identical emitters will be influenced by the constantly changing environment, which randomizes the phase of the excited state on the dephasing time scale, T_2. If T_2 is much smaller than the excited state lifetime T_1, the line width $\Gamma = (1/2\pi T_1 + 1/\pi T_2)$ will be much broader than that set by the lifetime limit T_1. For Ag:DNAs, T_1 is in the nanosecond range [52], corresponding to line widths in the μeV range, in the absence of dephasing.

When cooling down the ensemble, the aqueous solution freezes and becomes glassy. The emitters are immobilized in this inhomogeneous environment, in which local, microscopic variations in the medium shift the electronic energy levels of one emitter relative to another. So while the single-emitter line width could be reduced by an increase in the T_2 time at low tem-

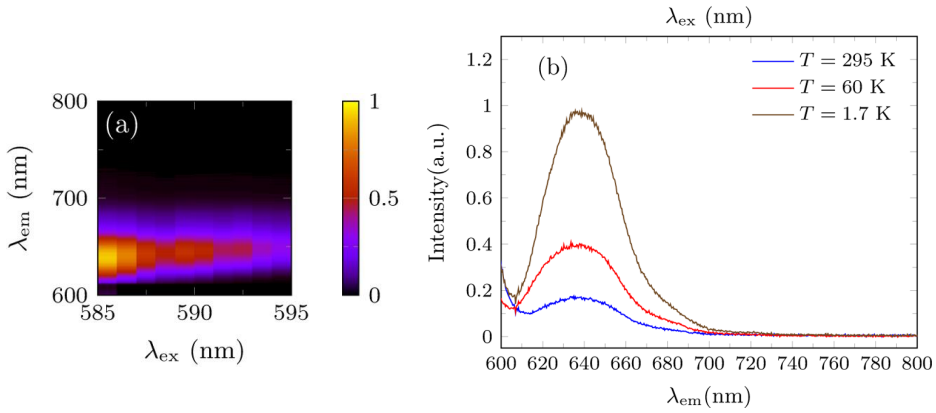

Figure 2.2: a) Emission intensity of an Ag:DNA1 ensemble at 1.7 K as a function of the excitation and emission wavelengths. Results for Ag:DNA2 were similar. b) Ensemble emission spectrum of Ag:DNA1 at different temperatures, excited at 585 nm. The width and position of the emission peak are only very weakly dependent on the temperature, indicating that thermal broadening effects are negligible in the ensemble. Nevertheless, the efficiency of the radiative path is seen to increase by a factor of 5.

peratures, the spectrum of a collection of emitters which experience different environments is inhomogeneously broadened.

The results of such ensemble measurements are shown in Figure 2.2 for Ag:DNA1. Results for Ag:DNA2 were similar. The excitation and emission spectra are plotted in Figure 2.2 a, where the emission intensity (color) is shown as a function of excitation wavelength (horizontal axis) and emission wavelength (vertical axis) at 1.7 K. Figure 2.2 b shows the emission spectra for three different temperatures of the same ensemble at a fixed excitation wavelength of 585 nm.

Figure 2.2 a shows that, when tuning the excitation wavelength at 1.7 K, the emission peak of the ensemble tends to shift in the same direction by the same amount. This is a signature of inhomogeneous (ensemble) broadening. Namely, as the excitation wavelength is detuned, the corresponding subensembles become more efficient at absorbing the laser light and will thus become brighter, and therefore, the ensemble will predominantly emit at a wavelength that is shifted accordingly.

The full width at half-maximum (fwhm) at 295 K in a glycerol solution is

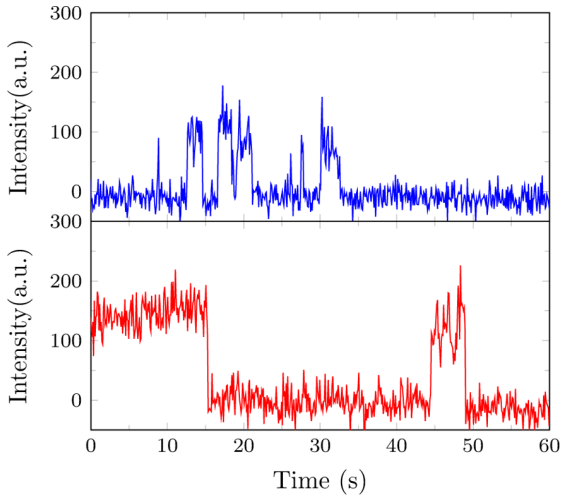

Figure 2.3: Emission intensity as a function of time, of two different Ag:DNA1 emitters embedded in PVA at room temperature, exposed to air. The fact that there are only two states, on and off, implies that we are indeed looking at single Ag:DNA emitters.

50 nm, and at 1.7 K, the fwhm is 41 nm, as seen in Figure 2.2 b. The 600 nm long-pass emission filter affects the measured line shape at the short-wavelength side. Integrating the area under the curves in Figure 2.2 b shows that the ensemble emission brightens by a factor of 2.3 from 300 to 59 K, and by a factor of 2.2 from 59 to 4 K.

The experiment was repeated for different concentrations of glycerol in the host medium, with no significant spectral differences. No additional broadening was observed as a function of excitation intensity, but at higher powers, the emitters did bleach in a very short time.

The aforementioned inhomogeneous broadening can be circumvented by studying individual emitters. For data at the single-emitter level, we preferred a host medium containing PVA rather than glycerol, as explained before. Thus, we spincoated Ag:DNA emitters in PVA onto the substrate, using low Ag:DNA concentrations to ensure average emitter separations well above the diffraction limit, enabling us to study them individually.

At first, we verify at room temperature that our sample has a suitable spatial distribution of emitters. While still at room temperature, with the sample exposed to air, blinking on the second time scale is observed, and

bleaching in about five minutes. We proceed to flush the sample space with He gas, which reduced both blinking and bleaching. We conclude that, on the second time scale, blinking and bleaching are caused by the presence of components in air, most likely oxygen. Typical blinking at room temperature in air can be seen in Figure 2.3, where the sudden jump from an on to off state, and vice versa, indicates that we are indeed only observing a single Ag:DNA emitter, instead of a small group of emitters lying within an area of the size of the diffraction limit.

Due to their limited brightness at room temperature, single molecule spectra were quite noisy, as can be seen in Figure 2.4 a. There, the spectrum of an individual Ag:DNA1 emitter is shown with an emission peak at 646 nm and a fwhm of 51 nm (0.15 eV). This is comparable to the fwhm of the ensemble at room temperature shown in Figure 2.2 b. The single-emitter spectra will be discussed further below.

After cooling down to 1.7 K, we again excite a wide area of the sample and record images, for different excitation wavelengths. The images reveal that the individual emitters become brighter at low temperature, that the peak excitation wavelength varies from emitter to emitter, and that the excitation spectrum is broad at the ~ 10 nm scale. This is visualized in Figure 2.5. The false-color image shown there is constructed from three different images, collected at 575, 585, and 595 nm and encoded as red, green, and blue, respectively. These three images are then superimposed, resulting in Figure 2.5. The varying colors show that different individual emitters have different excitation wavelengths. Emitters with mixed colors absorb at two or three of the mentioned excitation wavelengths, as can be found in the schematic on the left of Figure 2.5, and roughly indicates the large width of the excitation line for that emitter. Because the peak emission wavelengths lie outside the laser tuning range, it was not possible to determine excitation line widths, but in all cases, they appear to be well above 10 nm.

From such an image, we pick several emitters, and for each of those, we use a fast-steering mirror to direct the focused laser spot to excite only that single emitter, and record its emission spectrum. Such a single-emitter emission spectrum is shown in Figure 2.4 c, and can be compared to a typical emission spectrum at room temperature in Figure 2.4 a, and a spectrum at 223 K shown in Figure 2.4 b. There, it can be seen that on a single emitter level, and an integration time of 60 s, the spectral width of the emission at

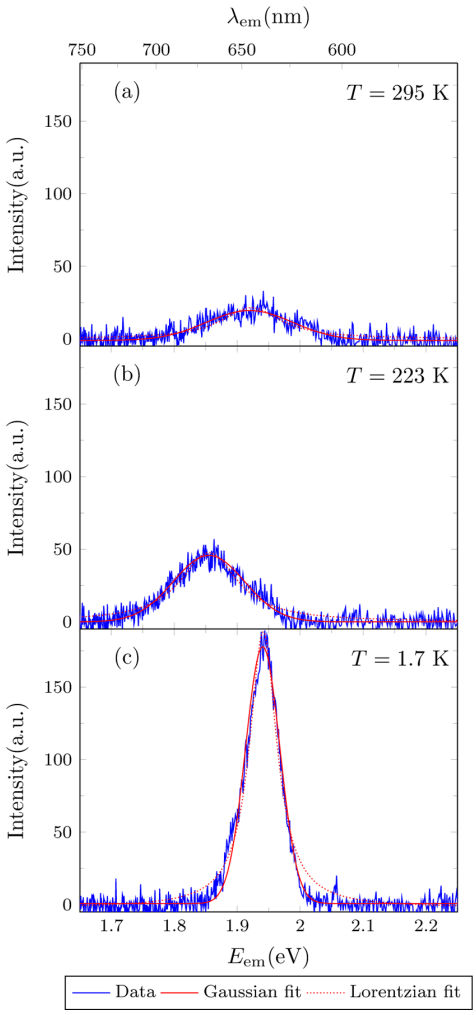

Figure 2.4: Emission spectra plotted versus photon energy of three different Ag:DNA1 emitters, with both Gaussian and Lorentzian fits. a) At room temperature, the single emitters are generally very dim, with an average fwhm of 50 nm or 0.15 eV. b) At 223 K, the brightness goes up. The spectrum shown here is of a different, individual emitter than the one from (a). As such, the position of the central peak is not related to temperature, but rather due to the difference in the individual emitters and their electronic environment, as discussed in the caption of Figure 2.7 and surrounding text. c) The spectrum of yet another individual Ag:DNA1 emitter, now at 1.7 K. As compared to the spectrum in (a), the brightness has increased by a factor of 5 and the line width has decreased to 23 nm or 0.070 eV for the specific emitter shown in (c). Averaging over 17 emitters, we find a fwhm of 26 nm or 0.079 eV at 1.7 K. The line shape is closer to Gaussian than Lorentzian, which is most apparent in the wings.

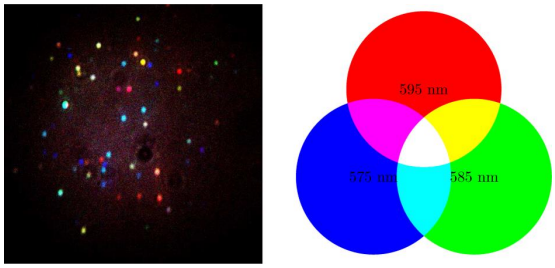

Figure 2.5: False-color image of the excitation dependence of emission from Ag:DNA1 emitters embedded in PVA. Results for Ag:DNA2 were similar. This left image consists of three superimposed CCD images: Excitation at 575 nm in blue, at 585 nm in green, and 595 nm in red, as schematically shown on the right. As such, the image illustrates (i) the spatial distribution, (ii) the variation of peak excitation wavelengths, as different emitters are indicated with different colors, and (iii) the $\sim$20 nm width of the absorption lines, as many emitters are mixed in color. Note that one or two emitters appear to be magenta-colored, i.e., they are bright at both 575 and 595 nm, but dim at 585 nm. This is due to the fact that they blinked during recording, and were mostly dark when recording the image at 585 nm. The size of the CCD image is 50 μm.

1.7 K has decreased by roughly a factor of 2, from 51 nm (0.15 eV) at room temperature to 26 nm (0.079 eV) at 1.7 K. Figure 2.4, where the spectra are plotted versus photon energy, clearly shows that a Gaussian profile fits better than a Lorentzian profile.

As discussed before, during cool-down we do not track the location of any given emitter continuously as a function of temperature. From the collection of individual emitters, we find that the average brightness at 1.7 K is, on average, a factor of 5.1 $\pm$ 0.9 higher than of an individual emitter at room temperature. This is consistent with the increase in brightness we found in the ensemble spectra, as seen in Figure 2.2. Additionally, this result is reminiscent of earlier work on 77-300 K ensemble emission spectroscopy of histidine-protected Au_{10} clusters [64], where the decrease in brightness with increasing temperature was attributed to an increase in the non-radiative energy loss rate, due to thermally activated trapping of electrons in surface states. The same mechanism may account for the dimming of emission with increasing temperature that we observe. Note, however, that the line widths we obtain here are much smaller than found in the ensemble studies of Au_{10}, in which

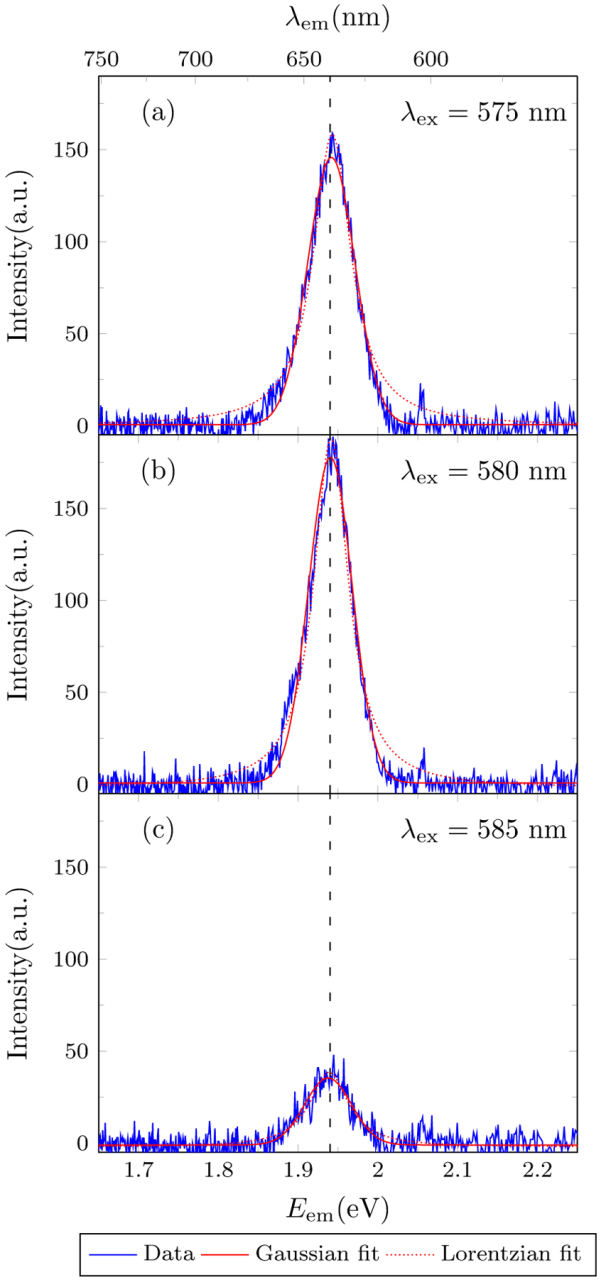

Figure 2.6: Emission spectra as a function of photon energy of the same Ag:DNA1 emitter at 1.7 K, for the excitation wavelengths (a) 575 nm, (b) 580 nm, and (c) 585 nm. The emission peak stays at 1.94 eV, or 639.1 nm, as indicated by the dashed line. The spectrum in (c) appears less bright, due to the fact that the emitter bleached during data acquisition.

the contribution of the inhomogeneous broadening to the line width was unknown.

As Figure 2.6 illustrates, (i) the single emitter has a broad excitation line and thus fluoresces for excitation for all three wavelengths, and (ii) the single emitter spectral shape does not depend on the excitation wavelength. As long as the individual emitter can be excited, its emission spectrum is a Gaussian shape with the same width, centered at the same spectral location. The specific emitter shown in Figure 2.6 is more efficiently excited at 580 nm than at 575 nm, and thus, the emission peak is stronger in Figure 2.6 b. Note, however, that the peak in Figure 2.6 c is much weaker due to the fact that the emitter bleached during data acquisition.

Across the population of Ag:DNA1 emitters in the field of view, the peak emission wavelength varies by tens of nm at 1.7 K (see Figure 2.7). The most 'blue' emitters that we found were centered around 620 nm, and the most 'red' emitters were centered at 670 nm. When averaging over multiple emitters, we find that the emission peak lies at 636 $\pm$ 17 nm (1.95 $\pm$ 0.05 eV). The variation in peak wavelength among individual emitters could be caused by local, nanoscale variations in the PVA embedding medium, such as local strain fields that deform Ag:DNA conformations and shift peak wavelengths. Another possible cause is that the different peak wavelengths correspond to slightly different structural isomers, e.g., with differences in binding sites on the DNA.

In contrast to the spread in emission peak locations, the single emitter line width varies relatively little across the population. At 1.7 K, we find a line width of 26 $\pm$ 4 nm (averaged over 17 emitters), corresponding to a line width of 79 meV. Thus, this large line width appears to be a property intrinsic to the Ag:DNA1 itself. Comparison to data on Ag:DNA2, which shows a substantially larger line width of 45 nm (124 meV), indicates that the line width is sensitive to the specific structure of the emitter.

Note that, for room-temperature data, the single-molecule spectra in Figure 2.4 a, with spin-coated PVA as the embedding medium, cannot be compared to the ensemble spectra in Figure 2.2 (bottom), with a glycerol solution as the embedding medium. Therefore, we repeated the single-molecule experiment in glycerol. At 1.7 K, the single emitter brightness was reduced by a factor of at least 3 relative to PVA, but the distribution of peak emission wavelengths, and the line widths, were similar. This indicates that the quantum

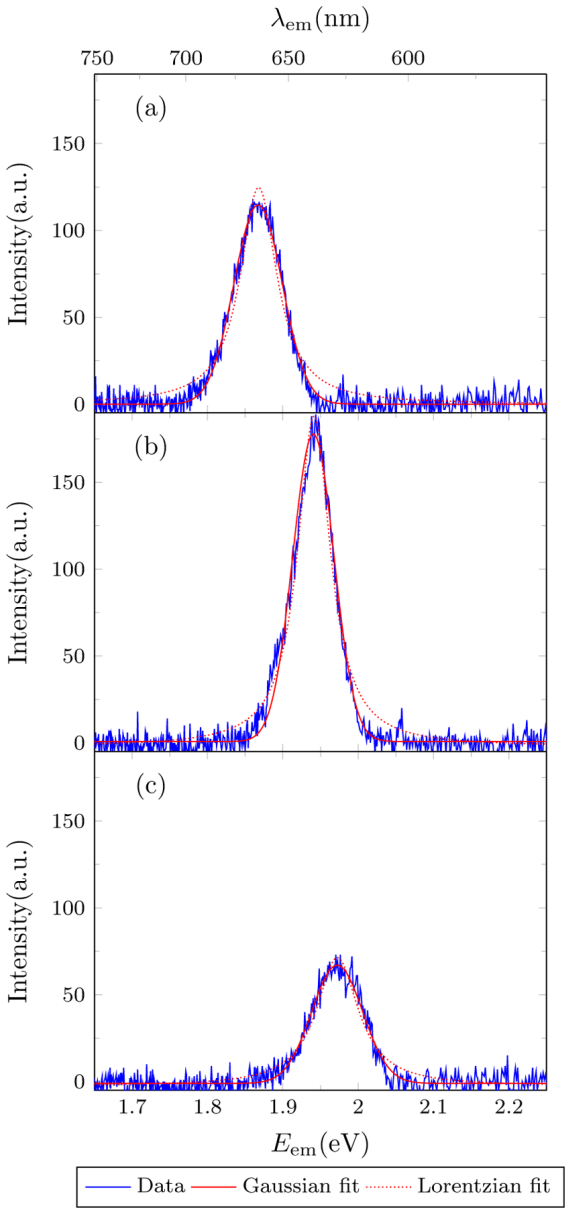

Figure 2.7: Emission spectra as a function of photon energy of three Ag:DNA1 emitters at 1.7 K excited at 585 nm, illustrating how the peak wavelength differs among different individual emitters. (a) and (c) lie toward shorter and longer wavelengths, respectively, when compared to an emitter closer to the mean (b). However, they all have a Gaussian profile with similar line widths. The spectra in (a) and (c) appear less bright than that in (b), most likely due to the fact that the peak of their absorption line is located farther from the laser excitation wavelength.

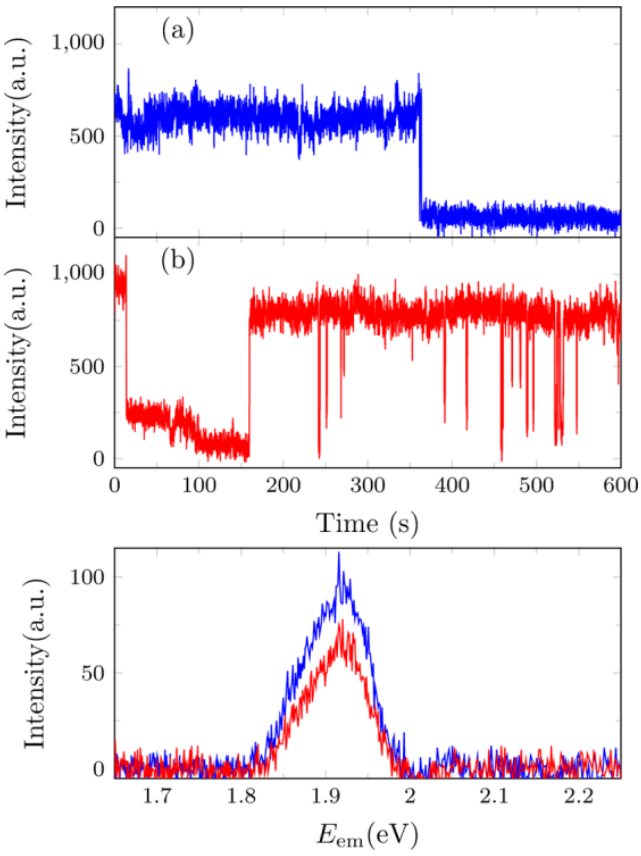

Figure 2.8: (a, b) Emission intensity as a function of time, of two Ag:DNA1 emitters embedded in PVA, at 1.7 K. a) Typical emitter, showing a single transition after 360 s, from the 'on' to the 'off' state. b) An atypical emitter, showing multiple on-off transitions, with many too short to be temporally resolved. c) Emission spectra of the aforementioned emitters. Spectrally, they are nearly identical, thus the slow blinking dynamics is apparently unrelated to the line width.

yield, and therefore the efficiency of the possible decay paths, can depend greatly on the chosen environment. In this case, it seems that, when comparing glycerol to PVA as a host medium, non-radiative decay is preferred over radiative decay.

Finally, we investigate the emission intensity as a function of time at low temperature, in order to study the dynamics on the second to minute time scale. In Figure 2.8 a, b we show the behavior of two single Ag:DNA1 emitters at 1.7 K embedded in PVA. Figure 2.8 a shows a single transition after 6 min, constituting bleaching. The fact that bleaching occurs in one step indicates that we were indeed observing one emitter. The stability of this emitter was representative of Ag:DNA1 at low temperature. The second emitter, Figure 2.8 b, was unusual in that it displayed blinking with short and long off-times. Considering that these emitters were spectrally quite similar, as shown in Figure 2.8 c, we attribute the differences in their blinking dynamics to the distinct, local microscopic environments. Regardless, the stability of the emitters at low temperature, as seen in Figure 2.8 a has improved when compared to the stability at room temperature, as shown in Figure 2.3.

2.4 Discussion

The main result of this work is that, on the single-emitter level, at low temperature, the Ag:DNA1 emission spectrum has a line width of 26 nm (79 meV) and shows a Gaussian profile. The factor of 5 difference in brightness at 1.7 K relative to room temperature can be explained by activation at higher temperatures of non-radiative decay, such as trapping. The behavior of Ag:DNA2 is very similar, with an even larger single-emitter line width of 45 nm. The question that remains is which mechanism causes this relatively broad spectral line at low temperatures.

Since the Ag:DNA solutions we study here are not chemically purified, we first comment on the fact that a given DNA strand can host different Ag:DNA species, with different spectral properties [9, 13, 65]. Of course, such Ag:DNA population heterogeneity affects the bulk solution measurements (Figure 2.1): different Ag:DNA complexes produce different emission peaks. However, population heterogeneity makes no contribution to the spectral properties of a single emitter, unless the individual emitter undergoes dynamic changes in bonding during the time required to collect the single emit-

ter spectrum. Such changes in bonding within a silver cluster are highly unlikely below 2 K [63]. Because calculations indicate that typical silver-base binding energies are $\sim$100 meV [65], it is also implausible that silver-base bonds would be breaking and reforming at the low temperatures we employ ($k_B T$ = 0.17 meV at T = 2 K).

We next consider the possibility that dynamic interactions of an individual emitter with low- nergy fluctuations in its local environment are the source of the large line width. In particular, for fluorescent molecules embedded in amorphous media, the coupling of electronic transitions to fluctuations of the medium can produce temporal wandering of optical transition energies [66]. This spectral diffusion persists at low temperatures due to the presence of low-energy localized modes in polymer and glassy embedding media.

Due to the fact that the averaging times required to measure emission spectra of single emitters are typically longer than time scales for spectral diffusion, emission lines are broadened. Therefore, unless other broadening mechanisms dominate the line width, we would expect to see evidence for spectral diffusion in single emitter spectra of Ag:DNAs. The properties of the single Ag:DNA spectra lead us to conclude that spectral diffusion is unlikely to account for the broad emission lines at low temperature. Namely, if the absorbance line were wandering over time, a change in the excitation wavelength would shift the emission peak, because the emitter would excite most efficiently during times when the absorbance peak wandered closest to the excitation wavelength. Instead, we find that the emission peak is independent of excitation wavelength (Figure 2.6). Moreover, spectral fluctuations that arise from conformational changes are implausible as a major source of broadening, because emitters embedded in glycerol exhibit the same line widths as those embedded in PVA. Glycerol forms a hard glass, and is known to immobilize emitters in more compact conformations, as has been observed with light-harvesting complexes [67]. In contrast, PVA consists of long polymer chains with many degrees of freedom. It seems unlikely that these two very different media would result in the same line width, if spectral diffusion were the broadening mechanism.

Another potential, nonintrinsic source for the broad emission lines of Ag:DNAs is the excitation of phonon modes of the embedding medium or of the DNA, via the emitters dipole moment. In general, electron-phonon

coupling results in emission of a low-energy phonon of the immediate surroundings of the emitter, simultaneous with the electronic transition. The width of the resulting emission feature, the phonon sideband, is governed by the phonon density of states in the emitters environment and the energy dependence of the electronphonon coupling. For polymer embedding media at low temperatures, diverse fluorescent molecules all exhibit phonon sidebands with widths of $\sim$10 meV [68–70] and line shapes that are asymmetrically broadened toward high energies. The $\sim$100 meV, Gaussian emission lines of single Ag:DNA emitters are qualitatively different, in line width and line shape.

Because the typical broadening mechanisms that arise from environmental couplings of fluorescent molecules do not appear to fit the behavior of Ag:DNAs, we consider whether the vibronic levels of the cluster itself might result in the observed line shape. Vibrational mode energies for silver clusters of tens of atoms are on the order of 100 cm^{-1} [71]. At low temperatures, transitions from the excited state to different vibronic levels of the ground electronic manifold would then give rise to a vibrational progression of narrow emission lines spaced by $\sim$10 meV ($\sim$ 3.5 nm, at 650 nm emission wavelength), resulting in an asymmetric comb-like shape. While the superposition of phonon sidebands from multiple vibronic transitions might result in a smooth rather than multi-peaked emission spectrum, we would still expect an asymmetric line shape at low temperatures, due to the absence of anti-Stokes processes. However, we observe a featureless, symmetric Gaussian line shape (see Figures 2.4 and 2.7).

From the above considerations, it appears that the optical transitions do not have a typical molecular character. While previous work on Ag:DNAs has assumed that the clusters are too small to support collective, plasmon-like excitations [10], we nevertheless turn to such a description in search of an explanation for the line width and shape. Comparison to results for small, bare silver clusters indeed suggests that the Ag:DNAs have collective, multi-electron excitations. Recent theoretical work has established the collective nature of the dominant optical excitation of Ag clusters composed of just $\sim$ 10 atoms [58], which display incipient plasmons at energies quite close to the value predicted by Mie theory, once the cluster shape is taken into account. Studies of smaller clusters of Na found a collective character in the low-energy excitations of Na_2, with just two free electrons [72]. For such a

phased collective excitation of multiple electrons, any process that kicks the phase of the collective excitation results in dephasing [73].

Because most quantum calculations for small clusters introduce the line width as a phenomenological constant, presently there is little information on what to expect for lifetimes in quantum-sized clusters. In much larger clusters, the decay of plasmons into single particle excitations (Landau damping) produces rapid energy relaxation together with dephasing, resulting in short excited-state lifetimes [60] that are incompatible with $T_1 \sim$ 1-5 ns, typical of Ag:DNAs [52]. However, in the quantum size regime, Landau damping can be strongly suppressed [60]. The few calculations that have treated dephasing at the fundamental level find complex dependencies of surface plasmon line widths on the size of spherical clusters [60], and dephasing line widths of $\sim$100 meV from surface plasmon coupling to zero-point shape fluctuations in Na_8 [59]. This latter mechanism leads to the expectation for strong dependencies of line widths on cluster shape. It also leads to line shapes with Gaussian tails, consistent with our results.

Our results, and comparison to previous work, indicate that dephasing in Ag:DNAs is quite sensitive to the specific cluster structure. In particular, the single-emitter line widths for Ag:DNA2 emitters are nearly twice as broad as for Ag:DNA1, even though their rather similar emission wavelengths ($\sim$ 620 nm, vs $\sim$ 680 nm) suggest similar overall structures. For ligand-free silver clusters frozen in noble gas matrices, ensemble measurements on size-selected clusters also indicate such structural sensitivity of the line width. Namely, fluorescence spectroscopy performed on small silver clusters (n = 2, 3) in gas matrices at room temperature [38, 74] suggest line widths around 80-160 meV, while ensembles of Ag_9 clusters frozen in Ar matrices showed very narrow emission lines ($\sim$2 meV) [41]. However, other measurements on absorption of Ag_{5-11} clusters embedded in an Ar matrix at low temperatures [75] also yielded line widths on the order of 125 meV, and spectral data on matrix-stabilized Ag_4 revealed a line width of 0.1 eV [40], which is comparable to our results. These empirical results indicate that, even in the relatively simple regime of unligated silver clusters, line widths appear to be strongly dependent on the details of the cluster structure. If we assume that the Ag_4 results [40] are not artificially broadened by the ensemble, this could indicate that, while the Ag:DNA emitters we studied contain a larger total number of silver atoms, they may have a similarly low degree of Ag

coordination.

These considerations lead us to believe that the smooth, Gaussian line shape is intrinsic to the Ag:DNA itself, and that dephasing of a collective, multiple electron excitation is the most likely broadening mechanism.

2.5 Conclusion

In summary, we have performed a low-temperature spectroscopic study on single fluorescent Ag:DNA emitters. We find that when a single emitter is cooled from 295 to 1.7 K, the brightness goes up by a factor of 5, while the line width decreases by a factor of 2. These results indicate that cooling increases the efficiency of the radiative decay channels, while reducing the number of non-radiative mechanisms such as electron-phonon scattering. The single emitter line width of 26 nm (0.079 eV) at low temperature for an individual emitter, which is more than half of the ensemble spectral width, corresponds to a dephasing time of 17 fs, which we suggest arises from dephasing of collective excitations. Considering the line width of 26 nm (0.079 eV) and the $\sim$ 300 nm ($\sim$ 1 eV) spectral range of Ag:DNA peak emissions identified to date, this corresponds to the availability of roughly 10 independent color channels to future labeling applications.